

6. Yu. A. Medvedev, B. M. Stepanov, and G. V. Fedorovich, "Pulsed function of streams of Compton electrons," in: Problems of the Metrology of Ionizing Radiations [in Russian], Atomizdat, Moscow (1976).
7. O. F. Evdokimov, "Multiple scattering of fast electrons in a gas in the presence of an electric field," Zh. Tekh. Fiz., 45, No. 3, 593-599 (1975).
8. A. V. Zhemerev, Yu. A. Medvedev, and B. M. Stepanov, "Pulsed current of electrons excited by  $\gamma$ -radiation in air," Atom. Energ., 41, No. 4, 268-269 (1976).
9. A. V. Grevich, "Theory of the effect of escaping electrons," Zh. Eksp. Teor. Fiz., 39, No. 5(11), 1296-1307 (1960).
10. S. C. Brown, Introduction to Electrical Discharges in Gases, Wiley (1966).
11. J. Dutton, "A survey of electron-swarm data," J. Phys. Chem. Ref. Data, 4, No. 3, 577-856 (1975).
12. Yu. P. Raizer, Laser Flash and the Propagation of Discharges [in Russian], Nauka, Moscow (1974).
13. L. E. Kline and Y. G. Siambis, "Computer simulation of electrical breakdown in gases: avalanche and streamer formation," Phys. Rev., 5, No. 2A, 794-805 (1972).

IONIZATION AND RECOMBINATION OF A MULTICHARGED PLASMA HEATED BY  
LASER RADIATION

A. N. Polyanchikov and V. S. Fetisov

UDC 533.95:621.375.826

Ionization and recombination processes taking place in a laser plasma during its heating up and subsequent cooling play an important role in the formation of the charge and energy spectra of the plasma ions [1, 2]. It appears that recombination during dispersion of the plasma does not lead to the total disappearance of the charged particles. The possibility of hardening the degree of ionization was shown theoretically for the first time in [3]. A subsequent study of the dispersion of a previously heated and ionized plasma [4-6] showed that the most effective hardening occurs at the periphery of the plasma bunch, i.e., where the rate of expansion of the plasma is the highest and the density is the lowest. However, in all these papers, the stage of heating up of the plasma by laser radiation has not been considered.

This paper is devoted to the numerical investigation of the dispersion of a multicharged plasma (aluminum and deuterium-carbon), subjected to the action of the radiation of a neodymium laser. The following inelastic processes are taken into consideration for the calculations: ionization by electron shock, photorecombination, ternary recombination at the ground level with an electron as the third particle, stopping absorption of radiation incident on the plasma, bremsstrahlung, electron thermal conductivity, and energy transfer between electrons and ions.

The dispersion of a continuous spherical bunch of multicharged plasma, in which the inelastic processes mentioned above occur, can be considered by means of the equations of gas dynamics, using the assumption of quasineutrality of the plasma. Breakdown of quasineutrality occurs at distances on the order of the Debye radius. For the plasma parameters used (density  $\sim 10^{22}$  cm<sup>-3</sup>, temperature  $\sim 10^2$ - $10^3$  eV), the Debye radius  $r_D \sim 10^{-6}$  cm, which is considerably less than the characteristic size of the plasma bunch  $R \sim 10^{-2}$  cm. Therefore, breakdown of quasineutrality can occur only close to the edge of the plasma, and at quite large dimensions of the bunch, the effect of the resulting electrical forces on the motion of the main bulk of the plasma is negligibly small [7]. The effect of the electric field can result, however, at distances of the mean free path of ions relative to ion-ion collisions  $l_{ii}$ . In fact, the self-consistent electric field originating even under the condition of quasineutrality leads to ions of different charges being accelerated differently in this field. At the same time ion-ion collisions create a strong friction which balances the velocities of the ordered motion of ions with different charges. This velocity balancing takes place over the whole volume of the plasma, with the exception of a small region of the order of  $l_{ii}$ , immediately

---

Moscow. Translated from Zhurnal Prikladnoi Mekhaniki i Tekhnicheskoi Fiziki, No. 6, pp. 9-15, November-December, 1978. Original article submitted October 25, 1977.

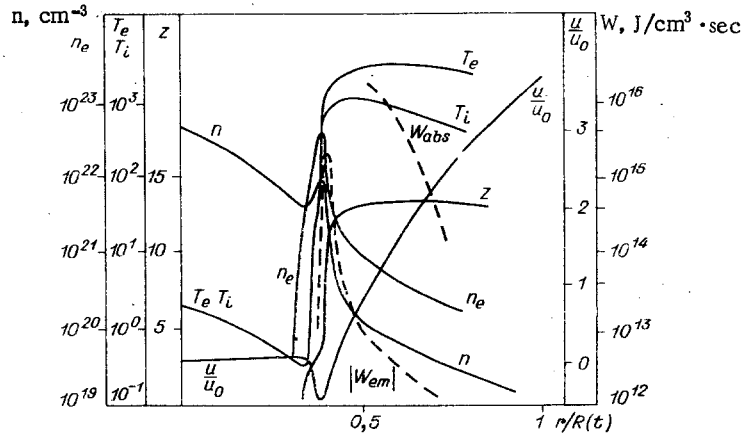


Fig. 1

adjacent to the edge. We shall consider the following plasma parameters: temperature of the electrons and ions  $T_e \sim 10^2 - 10^3$  eV and  $T_i \sim 10^2$  eV; ionization potential  $J(z) \sim 10^3$  eV; ionic charge  $z \sim 10$ ; density of atoms  $n \geq 10^{21}$   $\text{cm}^{-3}$ ; and radius of bunch  $R \sim 10^{-2}$  cm. Then, in the main bulk of the bunch  $l_{ii} \sim 10^{-7}$  cm, i.e.,  $l_{ii} \ll R$ , and the motion of the plasma can be considered in single-liquid approximation. It should be noted, however, that near the edge, because of the low plasma density,  $l_{ii}$  may prove to be on the order of the dimensions of the region of hardening of ions with a high charge ( $z \gg 1$ ), which would lead to separation of the charges according to velocity in this region, observed experimentally, for example, in [1]. This phenomenon has not been taken into account in our model.

We shall consider a plasma consisting of a mixture of ions of two kinds. The first kind consists of ions with a high nuclear charge  $z_m \gg 1$ , nuclear mass  $M_1$ , and atom density  $n_1$ . The other kind consists of ions with a nuclear charge equal to unity (deuterium), atomic mass  $M_2$ , and atom density  $n_2$ . Since we shall be considering mainly temperatures of  $\sim 10^2 - 10^3$  eV, it can be assumed that the deuterium is completely ionized. The solution of the problem will be conducted on the assumption that at each instant mainly ions of one charge are present at each point [8]. The concentration of ions and their ionization potentials will be considered as continuous functions of the ion charge  $z$ .

Thus, as a start, we shall take the following system of hydrodynamic equations, describing the dispersion of the two-component laser plasma:

$$\begin{aligned}
 Mn \left( \frac{\partial u}{\partial t} + u \frac{\partial u}{\partial r} \right) &= - \frac{\partial}{\partial r} (p_e + p_i), \\
 \frac{\partial n}{\partial t} + \frac{1}{r^2} \frac{\partial}{\partial r} (r^2 u n) &= 0, \\
 \frac{\partial p_e}{\partial t} + u \frac{\partial p_e}{\partial r} + \frac{5}{3} \frac{p_e}{r^2} \frac{\partial}{\partial r} (r^2 u) &= \frac{5}{3r^2} \frac{\partial}{\partial r} \left( r^2 \kappa \frac{\partial T_e}{\partial r} \right) + W_{abs} + W_{em} + W_0 - Q_{ie}, \\
 \frac{\partial p_i}{\partial t} + u \frac{\partial p_i}{\partial r} + \frac{5}{3} \frac{p_i}{r^2} \frac{\partial}{\partial r} (r^2 u) &= Q_{ie}, \quad \frac{\partial z}{\partial t} + u \frac{\partial z}{\partial r} = A_z,
 \end{aligned} \tag{1}$$

where  $u$  is the hydrodynamic velocity;  $p_e$  and  $T_e(p_i, T_i)$  are the pressure and temperature of the electrons (ions);  $z$  is the average charge of ions of the first kind;  $n = n_1 + n_2$  is the total density of atoms;  $M = M_1 \varphi_1 + M_2 \varphi_2$ ;  $\varphi_1 = n_1/n$  and  $\varphi_2 = n_2/n$  are the concentrations of atoms of the first and second kinds, respectively;  $\kappa$  is the coefficient of electron thermal conductivity; and  $A_z = \Gamma_1 - \Gamma_2 - \Gamma_3$  is the rate of change of the average charge of the plasma ions  $z$  due to inelastic processes. The expressions for the ionization rates by electron shock  $\Gamma_1$ , photorecombination  $\Gamma_2$ , and ternary recombination at the ground level  $\Gamma_3$  [9] have the following form

$$\begin{aligned}
 \Gamma_1 &= 5 \cdot 10^{-6} \frac{\xi n_e e^{-\frac{J(z+1)}{T_e}}}{J(z+1) T_e^{1/2} [1 + J(z+1)/T_e]}, \\
 \Gamma_2 &= 1.68 \cdot 10^{-14} \frac{\xi n_e J^2(z)}{T_e^{3/2} [1 + J(z)/T_e]}, \\
 \Gamma_3 &= 8.25 \cdot 10^{-28} \frac{\xi n_e^2}{J(z) T_e^2 [1 + J(z)/T_e]},
 \end{aligned}$$

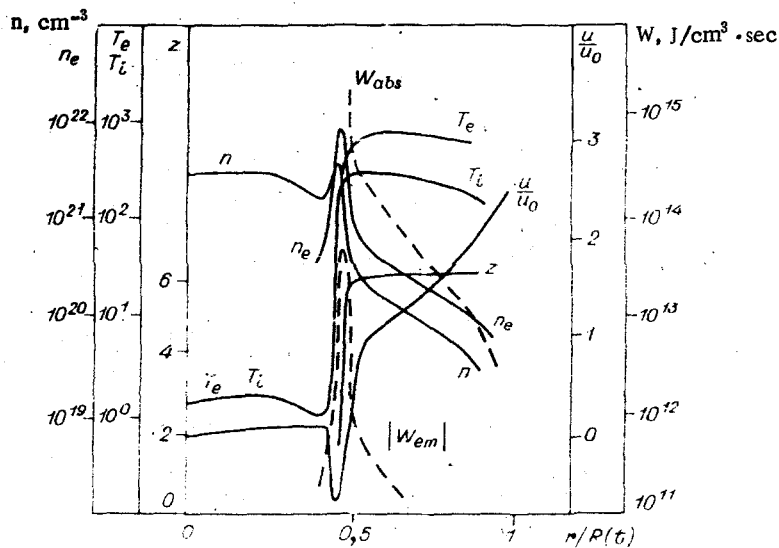


Fig. 2

where  $\xi$  is the number of valence electrons. The expression for the rate of ternary Pitaevskii-Gurevich recombination at a highly excited level with subsequent diffusions of the electron through the levels is not given here, although this process was also provided for in the program. This is because Pitaevskii-Gurevich recombination under these conditions does not make any contribution. Its characteristic time is  $\sim 3 \cdot 10^{-5}$  sec, which is much greater than the times of photorecombination ( $\sim 3 \cdot 10^{-10}$  sec) and ternary recombination at the ground level ( $\sim 10^{-8}$  sec). It can be seen from a comparison of the characteristic times that photorecombination plays the main role in the formation of the space distribution of the charge; however, ternary recombination at the ground level can introduce errors during expansion, when the plasma temperature falls to a value of  $\sim 10$  eV.

Absorption of laser radiation during dispersion of a multicharged plasma takes place mainly in consequence of the reverse stopping effect as a result of electron and ion collisions. In accordance with this, the magnitude of the light energy absorbed by the electrons  $W_{abs}$  is determined by the well-known formula  $W_{abs} = kq$ , where  $k = (v_{ei}/c)(n_e/n_c)[1 - (n_e/n_c)]^{-1/2}$  is the local coefficient of stopped absorption;  $q$  is the energy flux of the laser radiation;  $n_e = n(z\varphi_1 + \varphi_2)$  is the electron density;  $v_{ei}$  is the frequency of electron-ion collision;  $n_c = m\omega_0^2/4\pi e^2$  is the critical density ( $e$  is the charge, and  $m$  is the mass of the electron);  $c$  is the speed of light;  $W_{em} = -1.53 \cdot 10^{-25} n_e T_e^{1/2} n (z^2 \varphi_1 + \varphi_2)$  is the loss of energy to bremsstrahlung [10]; and  $W_0 = n\varphi_1 [J(z)\Gamma_3 - (3/2)T_e\Gamma_2 - J(z+1)\Gamma_1]$  is the change of energy of the electrons as a result of recombination and ionization. Bremsstrahlung and radiation during photorecombination freely leave the plasma, since the range of the radiation is  $\sim 1$  cm, which is much greater than the characteristic size of the plasma  $R \sim 10^{-2}$  cm;  $Q_{ie} = 2n(m/M)v_{ei}(T_e - T_i)$  is the rate of transfer of energy from the electrons to ions.

The system of equations (1) was replaced by finite-difference equations, which were integrated on a computer. In order to smear out discontinuities, an artificial viscosity was introduced into the calculations. The equations for  $p_e$  and  $p_i$  were solved by the sweep method.

Numerical calculations were carried out for the dispersion of a spherical, dense (aluminum or deuterium-carbon) target, heated by neodymium laser radiation with a frequency of  $\omega_0 = 1.78 \cdot 10^{15}$  sec $^{-1}$ . The density distribution of the atoms  $n_0$  and temperature  $T_{in} = 3$  eV at the initial instant  $t_{in}$  are assumed to be uniform. At a certain time ( $2 \cdot 10^{-8}$  sec) the plasma is dispersed without heating up. In this time, the rarefaction wave reaches the center of the bunch and density and temperature profiles are created. Similar profiles can be obtained by the vaporization of a solid target with a laser background or with a previous weak laser pulse. After this, the main laser pulse with a triangular shape is switched on (the origin of reference of the time  $t = 0$  is taken as the instant of the start of operation of the main pulse):

$$q(r = R_0, t) = \begin{cases} 2q_m \frac{t}{\Delta t}, & 0 \leq t \leq \frac{\Delta t}{2}, \\ 2q_m \frac{\Delta t - t}{\Delta t}, & \frac{\Delta t}{2} \leq t < \Delta t, \end{cases}$$

where  $R_0 = 10^{-2}$  cm is the radius of the focal spot. Thus, for  $t_{in} > 0$ , dispersion and heating up of the plasma takes place simultaneously.

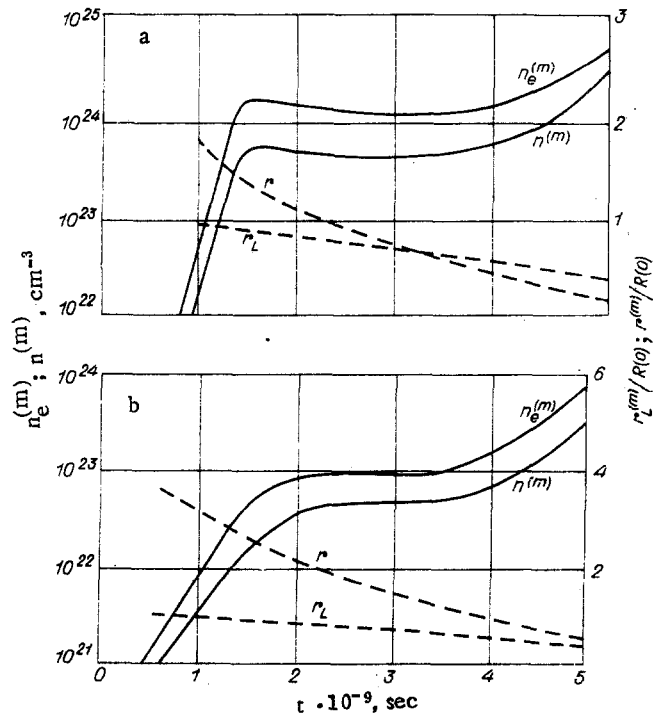


Fig. 3

The initial parameters of the plasma for  $t = t_{in}$  and the parameters of the laser pulse for the versions calculated have the following form: version 1 — aluminum plasma,  $n_0 = 5 \cdot 10^{22} \text{ cm}^{-3}$ ,  $R_0 = 10^{-2} \text{ cm}$ ,  $q_m = 4 \cdot 10^{14} \text{ W/cm}^2$ , and  $\Delta t = 2 \cdot 10^{-9} \text{ sec}$ ; version 2 —  $\text{CD}_2$  plasma,  $n_0 = 10^{23} \text{ cm}^{-3}$ ,  $R_0 = 10^{-2} \text{ cm}$ ,  $q_m = 10^{14} \text{ W/cm}^2$ , and  $\Delta t = 2 \cdot 10^{-9} \text{ sec}$ .

As the results of the calculations show, dispersion occurs in the following way. Absorption of the external radiation leads to heating up and ionization of the plasma. When the electron density reaches a critical magnitude, screening of the central part of the bunch occurs, and, consequently, the incident radiation can be absorbed only in the peripheral zone close to the edge of the plasma. The electron thermal conductivity is not in the state to equalize the temperature over the whole volume (characteristic time of thermal conductivity is  $\geq 10^{-9} \text{ sec}$ , i.e., on the order of or greater than the time of dispersion of  $\sim 10^{-9} \text{ sec}$  and the duration of the laser pulse), which leads to a spatial distribution of the hydrodynamic quantities shown in Figs. 1 and 2, where the curves are plotted for the instant  $t = 10^{-9} \text{ sec}$ , when the intensity of the laser radiation is a maximum. Figure 1 shows version 1 [ $u_0 = 2 \cdot 10^7 \text{ cm/sec}$ ,  $R(t) = 6.7 \cdot 10^{-2} \text{ cm}$ ]. Close to the edge, the temperature reaches a magnitude of  $\sim 10^3 \text{ eV}$ , whereas in the central part of the bunch the heating up is not experienced. The sharp boundary dividing these two regions and characterizing the enormous temperature and pressure gradient can be clearly seen. A shock wave is formed at this boundary, compression of the substance takes place, and a density spike to the atoms and electrons, which moves towards the center, originates. To the right of the shock wave, the charge of the plasma ions is close to the maximum. The front of the ionization wave almost coincides with the front of the shock wave, since the time of ionization  $\sim 10^{-11} \text{ sec}$  is much less than the hydrodynamic time of dispersion  $t_{hyd} \sim 10^{-9} \text{ sec}$ . In consequence of the high density, a bremsstrahlung spike also exists near the shock wave, somewhat displaced to the side of higher temperatures, i.e., to the edge of the plasma. The graphs of the hydrodynamic velocity shown in Figs. 1 and 2 show that the substance in the shock wave is moving toward the center. The converging shock wave causes compression of the substance in the central region, while at the periphery the density decreases because of dispersion. This pressure leads to the greater part of the mass of the plasma being concentrated in a small region near the center of the bunch. The motion of the density spike toward the center in Euler  $r$  and Lagrangian  $r_L$  coordinates and the variation of the spike density for versions 1 and 2 is shown in Fig. 3a, b, respectively;  $n^{(m)}$  and  $n_e^{(m)}$  are the maximum values of the density of the number of particles and the density of the electrons at the instant  $t$ ; and  $r^{(m)}$  is the position of the point with maximum density. The initial (at  $t = t_{in}$ ) coordinate of a specified particle of the plasma is taken as the Lagrangian coordinate. After its formation, the peak moves towards the

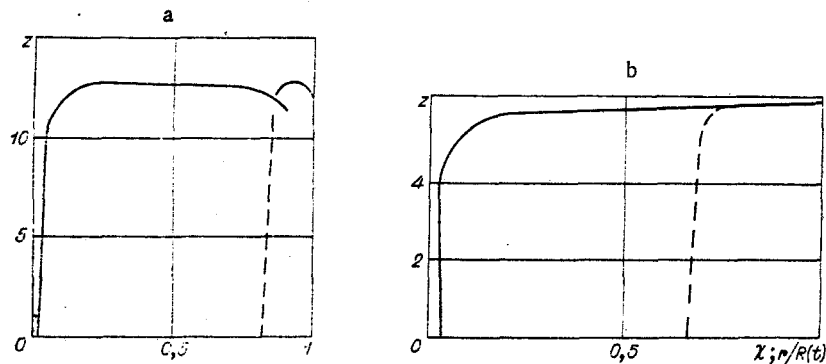


Fig. 4

center. Its density, first of all, varies weakly, but on approaching the center it increases and reaches its maximum value when the shock wave arrives at the center [ $\max n(r, t) = 6 \cdot 10^{24} \text{ cm}^{-3}$  for version 1 and  $\max n(r, t) = 10^{25} \text{ cm}^{-3}$  for version 2].

The high temperature at the periphery is the reason for the strong ionization, and the rapid fall of density in the presence of this high temperature prevents recombination, which leads to hardening of the degree of ionization in this region. As a result, a spatial distribution of the ion charge, which is asymptotic with respect to time, is obtained, as shown in Fig. 4a, b (version 1 and version 2, respectively); the solid and dashed lines correspond to the relations in the usual  $r$  and mass coordinates  $\left( \chi = \frac{\int_0^r nr^2 dr}{\int_0^{R(t)} nr^2 dr} \right)$ . The region of hardening occupies the greater part of the plasma volume, but the smaller part of the mass (for version 1, 15% of the plasma mass was exposed, while for version 2 it was 30%). Thus, the charge of the plasma ions, averaged over the volume, for version 1 is  $\langle z \rangle = 2.2$ , whereas at the periphery the aluminum ions are completely ionized and  $z(\chi \approx 1) = 13$  [for the  $\text{CD}_2$ -plasma,  $\langle z \rangle = 2$  and  $z(\chi \approx 1) = 6$ ]. This occurs because the major part of the mass of the plasma is found to be concentrated in a small region near the center of the bunch, where in consequence of the high density the plasma is completely recombined.

It should be noted that the stopping mechanism ensures almost total absorption of the laser radiation in a multicharged plasma, and for the versions calculated the coefficient of reflection was equal to zero during the whole time of operation of the laser pulse.

Thus, the investigation carried out has shown that the absorption of laser radiation in the vicinity of the edge of a plasma is due to hardening of the charge of the plasma ions in this region. The results obtained coincide qualitatively with the results of experimental observations [1, 2].

#### LITERATURE CITED

1. Yu. A. Bykovskii, N. N. Degtyarenko, V. F. Elesin, Yu. P. Kozyrev, and S. M. Sil'nov, "Mass-spectrometric investigation of a laser plasma," *Zh. Eksp. Teor. Fiz.*, **60**, 1306 (1971).
2. R. T. Rumsby and J. W. M. Paul, "Temperature and density of an expanding laser-produced plasma," *Plasma Phys.*, **16**, 247 (1974).
3. N. M. Kuznetsov and Yu. P. Raizer, "Recombination of electrons in a plasma, expanding in a vacuum," *Zh. Prikl. Mekh. Tekh. Fiz.*, No. 4, 10 (1965).
4. Yu. V. Afanas'ev and V. B. Rozanov, "Energy spectrum of multicharged ions in a laser plasma," *Zh. Eksp. Teor. Fiz.*, **62**, 247 (1972).
5. E. E. Lovetskii, A. N. Polyanchikov, and V. S. Fetisov, "Dispersion of a recombining plasma in a vacuum," *Zh. Tekh. Fiz.*, No. 5, 1025 (1974).
6. A. N. Polyanchikov and V. S. Fetisov, "Expansion in a vacuum of a multicharged plasma," *Zh. Tekh. Fiz.*, No. 11, 2337 (1975).
7. S. I. Braginskii, "Transfer phenomena in a plasma," in: *Problems of Plasma Theory* [in Russian], No. 1, Atomizdat, Moscow (1963).
8. Yu. P. Raizer, "Simple method of estimating the degree of ionization and thermodynamic functions of an ideal gas in the region of multiple ionization," *Zh. Eksp. Teor. Fiz.*, **36**, 1583 (1959).

9. L. A. Vainshtein, I. I. Sobel'man, and E. A. Yukov, Excitation Cross-Sections of Atoms and Ions by Electrons [in Russian], Nauka, Moscow (1973).
10. L. Spitzer, Jr., Physics of Fully Ionized Gases, Wiley-Interscience (1962).

#### EXPLOSIVE EMISSION IN GUIDED SLIDING DISCHARGES

S. I. Andreev, E. A. Zobov, and A. N. Sidorov

UDC 533.9+518.5+537.517

In [1] a method is proposed for controlling the development process of the discharge of a sliding spark along the surface of a film-type dielectric by the introduction into this surface of centers of emission consisting of chemical compounds with a low work function of the electrons.

The present article is devoted to an investigation of the nature of this means of control. Special experiments were set up which showed that the determining effect on the control is that of microexplosions of individual particles entering into the surface. The data of Fig. 1a (photograph of a sliding spark from the side) illustrate this assumption. The scattering of luminescing fragments of the emission centers (the visible diameter of the channel is approximately 0.5 mm) is clearly visible. The size of the fragments scattering with microexplosions is 10-100  $\mu\text{m}$ . The size of the individual particles entering into the surface is ~200-500  $\mu\text{m}$ . With projection of the axis of the channel of the discharge along the slit of the photorecorder (a streak camera), it is observed that microexplosions arise not only at the moment of the closing of the discharge gap (in Fig. 1b this moment is shown by an arrow), but also in incomplete stages of the discharge at moments corresponding to "surges" of the capacitance current [2] (Fig. 1b, 1 and 2).

It has been found that the visible intensity of the microexplosions depends to a considerable degree on the melting point of the metals of which the individual particles are made up. (Control is attained by the deposition of a surface film of varnish in which metallic powders are suspended). If part of the guiding band is deposited using titanium powder ( $T_{\text{mp}} = 1600^\circ\text{C}$ ), and if it is then prolonged using metallic calcium powders ( $T_{\text{mp}} = 850^\circ\text{C}$ ), then the development of a sliding spark in these sections differs in the intensity of the microexplosions. This is illustrated in Fig. 1c (the more intense region of luminescence relates to the part of the guiding band with calcium, while the less intense region relates to the part with titanium).

Up to the present time, microexplosions with metallic powders have been considered. As was shown in [1], there is guidance also with the use of dielectric powders. In this case, the microexplosions are more weakly expressed.

There is more effective guidance with the use of a mixture of barium oxide and graphite powders. In itself, graphite is not very effective for guidance (experiments with graphite have been made earlier [3]). In this mixture there is a sharp increase in the intensity of microexplosions from particles of graphite.

In our opinion, the explanation for this is the following. The presence of dielectric particles with a low work function (barium oxide) leads to a large number of electron cascades and streamer channels near the head of the developing leader. The graphite particles are current-collecting or conducting jumpers between the cascades. As a result, a large current flows through the graphite particles. This current leads to explosion of the conducting particles. The easier the material of the wire melts and the greater the current flowing through it, the more intense the explosive processes.

We must note one more special characteristic. As experiments have shown, a particularly high efficiency of the guidance can be obtained if the guiding band is bounded on both sides by bands with powders whose emission is minimal (for example, copper oxide  $\text{Cu}_2\text{O}$ ). In this case the development of a sliding spark takes place at the boundary between the two bands. The set of data obtained allows of the following hypothesis.

---

Leningrad. Translated from Zhurnal Prikladnoi Mekhaniki i Tekhnicheskoi Fiziki, No. 6, pp. 15-17, November-December, 1978. Original article submitted December 9, 1977.